Continuous Spectrum of Shear Alfvén Waves within Magnetic Islands

Alessandro Biancalani
Max-Planck-Institut für Plasmaphysik, Euratom Association, D-85748 Garching, Germany in collaboration with Max-Planck-Institut für Sonnensystemforschung, Katlenburg-Lindau, Germany

Liu Chen
Institute for Fusion Theory and Simulation, Zhejiang University, Hangzhou, People's Republic of China, and Department of Physics and Astronomy, University of California, Irvine, California 92697-4575, USA

Francesco Pegoraro
Department of Physics, University of Pisa, 56127 Pisa, Italy

Fulvio Zonca
Associazione Euratom-ENEA sulla Fusione, C.P. 65-I-00044-Frascati, Rome, Italy
(Received 25 March 2010; published 24 August 2010)

The radial structure of the shear Alfvén wave continuous spectrum is calculated inside the separatrix of a magnetic island. We find that, within a magnetic island, there is a continuous spectrum very similar to that of tokamak plasmas, where a generalized safety factor q can be defined and a wide frequency gap is formed, analogous to the ellipticity induced Alfvén eigenmode gap in tokamaks. This is due to the strong eccentricity of the island cross section. In this gap, a magnetic-island induced Alfvén eigenmode (MIAE) can exist as a bound state, essentially free of continuum damping, which can be resonantly excited by energetic particles and interact nonlinearly with the magnetic island. Because of the frequency dependence of the shear Alfvén wave continuum on the magnetic-island size, the possibility of utilizing MIAE frequency scalings as a novel magnetic-island diagnostic is also discussed.

DOI: 10.1103/PhysRevLett.105.095002 PACS numbers: 52.55.Tn, 52.35.Bj

Shear Alfvén waves (SAW) are electromagnetic plasma waves propagating with the characteristic Alfvén velocity $v_A = B/\sqrt{4\pi\varrho}$ (B is the magnetic field and ϱ the mass density of the plasma) as transverse waves along the magnetic field. In fusion plasmas, fast ions in the MeV energy range have velocities comparable with the typical Alfvén speed and can therefore resonantly interact with SAW and effectively exchange energy with the wave [1,2]. SAW in a nonuniform equilibrium are subject to collisionless dissipation, known as continuum damping [3–5], due to singular structures that are formed where the SAW continuum is resonantly excited. Because of magnetic field nonuniformities along the field lines in toroidal geometry, gaps appear in the SAW continuous spectrum [6] due to translational symmetry breaking, analogous to electrons traveling in a periodic lattice [1,2]. Discrete Alfvén eigenmodes (AE), with a frequency inside SAW continuum gaps [7], have a generally low instability threshold, being practically unaffected by continuum damping [1–5]. For this reason, understanding the continuous spectrum structure is important, due to the potential impact of AE stability on reaching the ignition condition for magnetically confined fusion plasmas.

The SAW continuous spectrum can be modified by the interaction with low-frequency MHD fluctuations [8], such as magnetic islands, which are formed when the original sheared equilibrium magnetic field lines break due to nonideal effects (in particular finite resistivity) and reconnect with different magnetic topology [9]. We model the magnetic island as a straight flux tube with a noncircular cross section [10]. Therefore, we neglect toroidicity effects on poloidal mode coupling; however, we do take into account the low-frequency gap in the SAW continuum due to the effects of geodesic curvature and finite compressibility [11–13].

We start our analysis by considering a tokamak geometry where R_0 is the major radius of the torus. The equilibrium is made of an axisymmetric tokamak magnetic field with a component $B_{\rm tor}$ in the toroidal direction ζ_T and a component $B_{\rm pol}$ in the poloidal direction θ_T, plus a helical perturbation $B_{\rm rad}$ in the radial direction r_T, generating a magnetic island. The subscript T denotes straight **B** field line tokamak coordinates. We consider the region in the proximity of the magnetic-island rational surface with minor radius r_0 and $q_T = q_0 = m_{\rm isl}/n_{\rm isl}$, where $m_{\rm isl}$ and $n_{\rm isl}$ are, respectively, the poloidal and toroidal mode numbers of the magnetic-island perturbation, and $q_T = r_T B_{\rm tor}/(R_0 B_{\rm pol})$ is the safety factor. The *constant-ψ* approximation is adopted, assuming that the magnetic-island perturbation has the form $B_{\rm rad} = B_{\rm isl}\sin u$, depending on the coordinate $u = n_{\rm isl}(\zeta_T - q_0\theta_T)$ only. The X points of the magnetic island are at $(q_T - q_0, u) = (0, 0)$ and $(0, 2\pi)$ and the O point at $(0, \pi)$. The magnetic flux surfaces of this equilibrium are labeled by $\psi = (q_T - q_0)^2/2 + M(\cos u + 1)$. M is a constant $M = (q_0|s|/n_{\rm isl}) \times (B_{\rm isl}/B_{\rm pol,0})$, determined by the condition $\boldsymbol{\nabla}\psi \cdot \boldsymbol{B} = 0$, where s is the magnetic shear and $B_{\rm pol,0}$ is the poloidal magnetic field evaluated at the rational surface $q_T = q_0$.

Here, the region inside the magnetic island is a straight flux tube with length $2\pi Z_0 = 2\pi\gamma q_0 R_0$, with ζ the translational symmetry coordinate, ψ the label of nested flux surfaces, $\gamma = \sqrt{1 + \varepsilon_0^2/q_0^2}$, and $\varepsilon_0 = r_0/R_0$. The magnetic axis and island O point are at $\psi = 0$, while the separatrix is labeled by $\psi = \psi_{\rm sx} = 2M$. The complete set of cylinderlike coordinates (ρ, θ, ζ) is defined by radial-like and anglelike coordinates given by

$$\rho = \frac{r_0}{q_0 s}\sqrt{2\psi}, \qquad \theta = \arccos[\sqrt{M(\cos u + 1)/\psi}]. \quad (1)$$

With these definitions, the magnetic axis is at $\rho = 0$ and the separatrix radius is $\rho = \rho_{\rm sx}$, which corresponds to the magnetic-island half-width $W_{\rm isl}$, given by the Rutherford formula [14]:

$$\frac{W_{\rm isl}}{r_0} = 2\sqrt{\frac{B_{\rm isl}}{q_0 s n_{\rm isl} B_{\rm pol,0}}} = \frac{\rho_{\rm sx}}{r_0} = \frac{2}{q_0 \gamma n_{\rm isl}}\sqrt{1-e},$$

with e defined below in this paragraph. The angle θ is defined in the domain $(0, \pi/2)$ and extended to $(0, \pi)$ by reflection symmetry with respect to $\theta = \pi/2$, with values $0, \pi$ at the rational surface $q = q_0$. Further extension to $(0, 2\pi)$ is obtained by reflection symmetry for $\rho \leftrightarrow -\rho$. We also point out that the flux surface's cross section in the (ρ, θ) plane and in the proximity of the O point is an ellipse, with eccentricity $e = 1 - M n_{\rm isl}^2 \gamma^2/s^2$. Typical magnetic islands in tokamak experiments have values of eccentricity close to $e \simeq 1$.

In the cylinderlike coordinates (ρ, θ, ζ) defined inside the magnetic island, the contravariant *physical* components of the equilibrium magnetic field are

$$B_{\rm ph}^{\rho} = 0, \qquad B_{\rm ph}^{\theta} = B_{\rm ph,0}^{\theta}\sqrt{a}\rho, \qquad B_{\rm ph}^{\zeta} = B_0.$$

Here $B_{\rm ph,0}^{\theta} = \varepsilon_0|s|B_0/(q_0 r_0 \gamma^2)$ is the value of $B_{\rm ph}^{\theta}$ at $\rho = 1$, $\theta = \pi/2$, where $B_0 = \gamma B_{\rm tor}$. The function a is defined as $a = \sin^2\theta + \cos^2\theta(1-e)F^2$, with $F = \sqrt{1 - x^2\cos^2\theta}$ and $x = \rho/\rho_{\rm sx}$. The contravariant physical components of a vector $\boldsymbol{V}$ on a basis $\{\boldsymbol{g}_r, \boldsymbol{g}_\theta, \boldsymbol{g}_\zeta\}$ are defined here as the contravariant components rescaled with the length of the correspondent basis vector, e.g., $V_{\rm ph}^{\rho} = V^{\rho}|\boldsymbol{g}_\rho|$. The safety factor q can be defined inside the magnetic-island flux tube as the average of $Q = \rho B_0/(Z_0 B^\theta)$ over θ, with $B^\theta = B_{\rm ph}^{\theta} F\sqrt{1-e}/(\sqrt{a}\rho)$; i.e.,

$$q = \frac{2}{\pi}\frac{\gamma}{|s|\sqrt{1-e}}K(x), \quad (2)$$

where we have introduced the complete elliptic integral of the first kind $K(x) = \int_0^{\pi/2} d\theta/F$. A similar definition was given in Ref. [15]. The result, normalized to the minimum value $q(x=0)$, is shown in Fig. 1. We see that $q(x)$ has a singular behavior near the separatrix $x = 1$, since B^θ vanishes at $\rho = \rho_{\rm sx}$, $\theta = 0, \pi$. This feature is due to the X points and is analogous to safety factor profiles in diverted tokamak plasmas.

Given the three-dimensional plasma equilibrium defined above, we want to study the shear Alfvén wave propagation near the resonant flux surfaces where the energy is absorbed by continuum damping; therefore, we focus on the dynamics of modes that are characterized by radial singular structures. The linear equation for radially localized shear Alfvén modes in a compressible nonuniform tokamak plasma can be written in the form [11]:

$$\frac{\omega^2}{\omega_A^2}\nabla_\perp^2\phi + Z_0^2\nabla_\parallel\nabla_\perp^2\nabla_\parallel\phi - \frac{\omega_{\rm BAE\ CAP}^2}{\omega_A^2}\nabla_\perp^2\phi = 0, \quad (3)$$

where $\omega_A = v_A/Z_0$. The frequency of the low-frequency SAW continuum accumulation point (CAP), delimiting the frequency gap of the beta induced Alfvén eigenmode (BAE), is defined as [11–13]

$$\omega_{\rm BAE\ CAP} = \frac{1}{R_0}\sqrt{\frac{2T_i}{m_i}\left(\frac{7}{4} + \frac{T_e}{T_i}\right)}, \quad (4)$$

where T_i and T_e are the ion and electron temperatures, and m_i is the ion mass. Here, we focus on frequencies higher than $\omega_{\rm BAE\ CAP}$ and consistently neglect kinetic effects associated with wave-particle resonances [13]. The operators $\nabla_\parallel$ and $\nabla_\perp$ are parallel and perpendicular gradients with respect to the equilibrium magnetic field.

Now, we write the equation for radially localized shear Alfvén modes, Eq. (3), in the cylinderlike coordinates introduced above. The parallel and perpendicular differential operators have the following form:

$$Z_0\nabla_\parallel = \sqrt{M}n_{\rm isl}F\frac{\partial}{\partial\theta} + \frac{\partial}{\partial\zeta}, \qquad \rho_{\rm sx}^2\nabla_\perp^2 = a\frac{\partial^2}{\partial x^2},$$

and the boundary conditions of the problem are periodicity

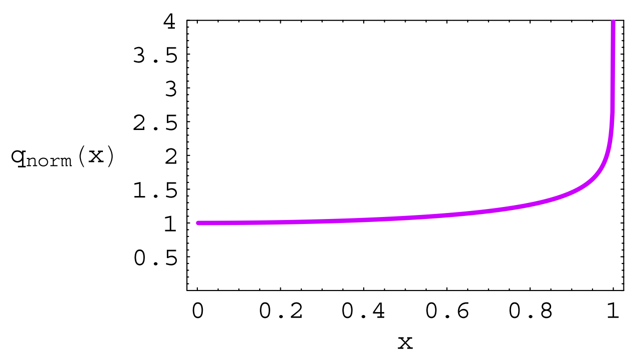

FIG. 1 (color online). The safety factor inside a magnetic island, normalized to $q(0) = 1/(\sqrt{M}n_{\rm isl}) = \gamma/(|s|\sqrt{1-e})$. For typical magnetic islands, $1 - e < 10^{-2}$ and we have $q(0) > 10$.

conditions in θ and ζ on 2π circles. Moreover, using the symmetry of the equilibrium in the ζ coordinate, we can write the general solution as $\phi = \hat{\phi}(x, \theta)\exp(-\mathrm{i}n\zeta)$, where n is the mode number in the ζ direction.

The problem we are considering is greatly simplified if we change coordinates from (ρ, θ, ζ) to a field aligned set of coordinates (ρ, θ, ξ), where $\xi = \zeta - \chi(x, \theta)$, and $\chi = (\sqrt{M}n_{\rm isl})^{-1}\int_0^\theta d\theta'/F(x, \theta')$ is the normalized incomplete elliptic integral of the first kind. In fact, we have $\boldsymbol{B}\cdot\boldsymbol{\nabla}\xi = 0$, and the parallel derivative takes the simple form $Z_0\boldsymbol{\nabla}_\parallel = \sqrt{M}n_{\rm isl}F\partial/\partial\theta$. Finally, Eq. (3) is written in the form of an eigenvalue problem:

$$\left[\frac{\Omega^2}{Mn_{\rm isl}^2} + \frac{F}{a}\frac{\partial}{\partial\theta}aF\frac{\partial}{\partial\theta}\right]\tilde{\phi}'' = 0, \qquad (5)$$

where $\Omega^2 = (\omega^2 - \omega^2_{\rm BAE\,CAP})/\omega_A^2$ is the eigenvalue, and $\tilde{\phi}'' = (\partial^2\hat{\phi}/\partial^2 x)\exp(-\mathrm{i}n\chi)$ is the eigenfunction. The boundary condition $\hat{\phi}''(\theta = 0) = \hat{\phi}''(\theta = 2\pi)$ now reads $\tilde{\phi}''(\theta = 0) = \tilde{\phi}''(\theta = 2\pi)\exp(2\pi\mathrm{i}nq)$, with the safety factor q defined in Eq. (2). We note that, in the case of small eccentricity $e \ll 1$, and close to the O point $x \simeq 0$, we have $a = F = 1$ and Eq. (5) reduces to the problem in cylindrical geometry: $\Omega^2 = Mn_{\rm isl}^2(nq - m)^2$, where m is the poloidal mode number.

The equation for SAW continuous spectrum written in the form of an eigenvalue problem in the coordinates (ρ, θ, ξ), as in Eq. (5), is an ordinary differential equation in one variable, θ, where the radial position x is treated as a parameter. It can be solved numerically, with a shooting method code for each position $0 < x < 1$, giving the continuous spectrum $\Omega^2(x)$ as the result. In Fig. 2, we show the result for the case $e \ll 1$, where we consider continuum modes with $n = 10$. We choose typical values for the equilibrium parameters, $q_0 = 2$, $s = 1$, $\varepsilon_0 = 0.1$, $n_{\rm isl} = 1$. In this case, we see that near the O point, $x \simeq 0$, the result of the cylindrical geometry is recovered. On the other hand, for $x \sim 1$, the flux surfaces have a noncircular cross section and therefore the modes with different m numbers are coupled. This mechanism creates a gap in the spectrum analogous to the ellipticity induced Alfvén eigenmode gap in tokamaks [16], dubbed here as magnetic-island induced AE (MIAE) gap. We repeated the calculation for a magnetic island with a typical size, $M = 10^{-2}$, using the same equilibrium parameters. This corresponds to $W_{\rm isl} \simeq \sqrt{1 - e}r_0 = 0.1r_0$, which is the order of magnitude of a saturated magnetic island in tokamaks. For this case, we considered modes with $n = 1$. The continuous spectrum structure, shown in Fig. 3, is the same as for $M = 1$, but in this case we obtain a much wider MIAE gap. This is due to the fact that flux surfaces of a typical magnetic island have a high eccentricity, which strongly couples modes with different m numbers. The MIAE gap central frequency is proportional to the magnetic-island half-width:

$$\Omega_{\rm MIAE} = \sqrt{M}n_{\rm isl} = \frac{q_0 s n_{\rm isl}}{2}\frac{W_{\rm isl}}{r_0}. \qquad (6)$$

For typical tokamak plasma parameters, $\omega^2_{\rm BAE\,CAP}/\omega_A^2 \sim \beta q_0^2$, with β denoting the ratio between plasma and magnetic pressures. Therefore, finite compression BAE frequency gap and magnetic-island induced MIAE gap are of comparable size when $M \sim \beta q_0^2$, i.e., for a typical saturated magnetic-island size in tokamaks. A gap analogous to the toroidicity induced Alfvén eigenmode gap [7,17] is not found here, because we consider a straight

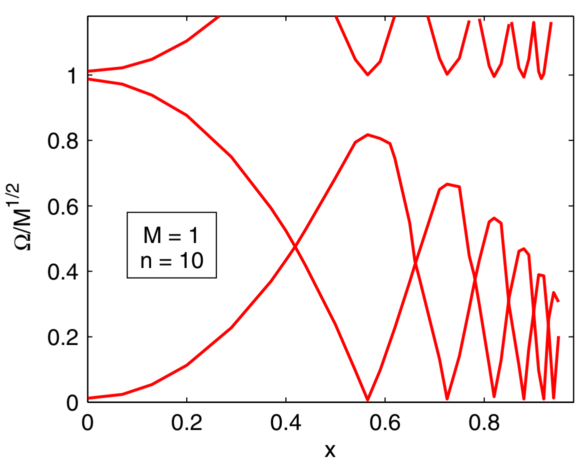

FIG. 2 (color online). Continuous spectrum $\Omega(x)$ for the small eccentricity case, $e \ll 1$, corresponding to $M \simeq 1$, plotted versus the radial position inside the island. Typical values of the equilibrium parameters have been chosen and $n_{\rm isl} = 1$. The O point is at $x = 0$ and the separatrix at $x = 1$. Modes with $n = 10$ are considered. The MIAE gap is found at frequencies $\Omega \sim \sqrt{M}n_{\rm isl}$.

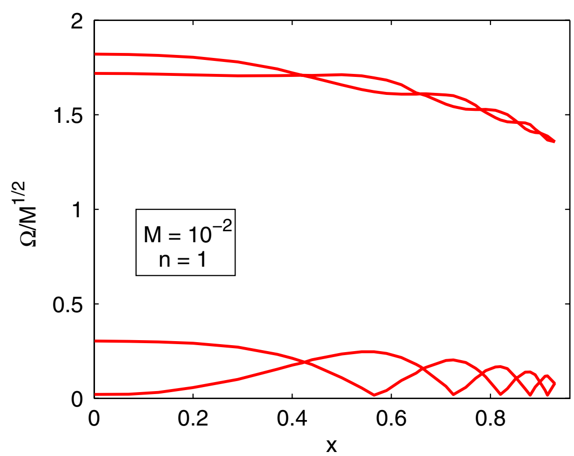

FIG. 3 (color online). Continuous spectrum $\Omega(x)$ for $n = 1$ and a typical size magnetic island: $M = 10^{-2}$, corresponding to $e \simeq 0.99$. In this case, the structure of the continuous spectrum is the same as for $M = 1$, but the MIAE gap is much wider. This implies that a wide range of frequencies exists, where modes contained within the magnetic island are not affected by continuum damping.

flux tube model, neglecting the effect of curvature coupling among different m numbers. Nevertheless, such a toroidal MIAE gap is expected to be present inside magnetic islands, at frequencies lower than the frequencies of the ellipticity MIAE gap. Its gap width can be estimated by substituting v_A with $v_A/(1 + \varepsilon_0 \cos\theta_T)$ in Eq. (3). This gives a multiplication factor $(1 + 2\varepsilon_0 \cos\theta_T)$ to the first and third terms of Eq. (3) (ε_0 is supposed to be small), and consequently to the first term of Eq. (5). Therefore, analogously to the theory of toroidicity induced AE, we expect to have a toroidicity induced gap within a magnetic island, with a width of the order of $\Delta\Omega^2 \simeq M n_{\rm isl}^2 \varepsilon_0$. The magnetic island also has a modulation in the tokamak toroidal direction, given by the number $n_{\rm isl}$. This helicity of the flux tube is neglected here and is expected to weakly couple modes of the SAW continuous spectrum with different n, analogously to the case of stellarators. These effects are not expected to qualitatively modify the MIAE gap and will be investigated in a different work as further extension of the present theory.

In summary, we have found that there exists a SAW continuous spectrum within a magnetic island, similar to that calculated in tokamak equilibria. In particular, a typical size magnetic island is shown to produce a wide gap in the continuous spectrum, labeled here as MIAE gap. Note that MIAE can exist as bound states within the island, essentially free of continuum damping, provided that plasma equilibrium effects and free energy sources can drive and bind them locally [4]. Here, we emphasize the analogy between the equilibrium inside a magnetic island and the tokamak equilibrium, and, consequently, the analogies between AE within the magnetic islands (MIAE) and the well-known AE in tokamaks. Given that plasma equilibrium nonuniformities and wave resonant interactions with energetic particles provide, respectively, frequency shift and mode drive [1,2], the MIAE peculiarity resides in the corresponding SAW continuous spectrum dependence on the magnetic-island size.

This result has important implications to the study of the dynamics and stability properties of a magnetic island. In fact, the presence of MIAE inside a magnetic island could modify the equilibrium profiles and nonlinearly affect the magnetic-island growth. On the other hand, MIAE could nonlinearly interact with energetic particles and affect their redistribution in the proximity of the magnetic-island rational surface. This process would add on the redistribution of fast ion population near a magnetic-island rational surface, caused in part by the radial magnetic field due to the magnetic island itself [18]. Therefore, adding the effect of MIAE can help to better understand fast particle dynamics in the presence of a magnetic island and explain the possible discrepancies between measured fast ion redistributions and theoretical predictions.

We have also shown that the frequency of the ellipticity MIAE gap is proportional to the magnetic-island width [see Eq. (6)]. This suggests the possibility of using the MIAE frequency scalings as a novel magnetic-island diagnostics in a fashion similar to other commonly used Alfvén spectroscopy techniques [19–21]. In fact, by detecting MIAE inside the island and measuring their frequency, one has indirect information on the magnetic-island size. Unlike in the BAE case, the radial MIAE localization at the center of the island makes them difficult to detect by external measurements, and makes the use of internal fluctuation diagnostics, such as electron cyclotron emission and soft x rays, necessary.

This work was supported by the Euratom Communities under the contract of Association between EURATOM/ENEA and in part by PRIN 2006 and CREATE, as well as by DOE Grants No. DE-FG02-04ER54736 and No. DE-FC02-04ER54796, and by the NSF Grant No. ATM-0335279. Part of this work was done while one of the authors, A. B., was at the University of Pisa, in collaboration with University of California, Irvine, and Centro Ricerche ENEA Frascati, which are gratefully acknowledged for the hospitality. One of the authors, A. B., would also like to thank Andreas Bierwage for valuable suggestions in writing the shooting method code. Useful discussions with C. Di Troia, I. Chavdarovski, X. Wang, and P. Porazik are also acknowledged.

[1] F. Zonca *et al.*, Plasma Phys. Controlled Fusion **48**, B15 (2006).
[2] L. Chen and F. Zonca, Nucl. Fusion **47**, S727 (2007).
[3] H. Grad, Phys. Today **22**, No. 12, 34 (1969).
[4] A. Hasegawa and L. Chen, Phys. Rev. Lett. **32**, 454 (1974).
[5] L. Chen and A. Hasegawa, Phys. Fluids **17**, 1399 (1974).
[6] C. E. Kieras and J. A. Tataronis, J. Plasma Phys. **28**, 395 (1982).
[7] C. Z. Cheng *et al.*, Ann. Phys. (Leipzig) **161**, 21 (1985).
[8] P. Buratti *et al.*, Nucl. Fusion **45**, 1446 (2005).
[9] H. P. Furth *et al.*, Phys. Fluids **6**, 459 (1963).
[10] A. A. Tuccillo *et al.*, Nucl. Fusion **49**, 104013 (2009).
[11] M. S. Chu *et al.*, Phys. Fluids B **4**, 3713 (1992).
[12] A. D. Turnbull *et al.*, Phys. Fluids B **5**, 2546 (1993).
[13] F. Zonca *et al.*, Plasma Phys. Controlled Fusion **38**, 2011 (1996).
[14] P. H. Rutherford, Phys. Fluids **16**, 1903 (1973).
[15] K. Swartz and R. D. Hazeltine, Phys. Fluids **27**, 2043 (1984).
[16] R. Betti and J. P. Freidberg, Phys. Fluids B **3**, 1865 (1991).
[17] C. Z. Cheng and M. S. Chance, Phys. Fluids **29**, 3695 (1986).
[18] M. Brüdgam, Ph.D. thesis, TU München, 2010.
[19] S. D. Pinches *et al.*, Plasma Phys. Controlled Fusion **46**, B187 (2004).
[20] B. Breizman *et al.*, Phys. Plasmas **12**, 112506 (2005).
[21] F. Zonca *et al.*, Nucl. Fusion **49**, 085009 (2009).